Use of photoactivation and photobleaching to monitor the dynamic regulation of E-cadherin at the plasma membrane

Cell Adhesion & Migration 4:4, 491-501; October/November/December 2010; © 2010 Landes Bioscience

Use of photoactivation and photobleaching to monitor the dynamic regulation of E-cadherin at the plasma membrane

Marta Canel,[1,*] Alan Serrels,[1] Kurt I. Anderson,[2] Margaret C. Frame[1] and Valerie G. Brunton[1]

[1]Edinburgh Cancer Research Centre; Institute of Genetics and Molecular Medicine; University of Edinburgh; Edinburgh, UK;
[2]Beatson Institute for Cancer Research; Glasgow, UK

Key words: E-cadherin, adherens junctions, plasma membrane, protein dynamics, photoactivation, photobleaching

Abbreviations: AJs, adherens junctions; GFP, green fluorescence protein; PAGFP, photoactivatable GFP; FRAP, fluorescence recovery after photobleaching; PA, photoactivation

The dynamic control of E-cadherin is critical for establishing and maintaining cell-cell junctions in epithelial cells. The concentration of E-cadherin molecules at adherens junctions (AJs) is regulated by lateral movement of E-cadherin within the plasma membrane and endocytosis. Here we set out to study the interplay between these processes and their contribution to E-cadherin dynamics. Using photoactivation (PA) and fluorescence recovery after photobleaching (FRAP), we were able to monitor the fate of E-cadherin molecules within the plasma membrane. Our results suggest that the motility of E-cadherin within and away from the cell surface are not exclusive or independent mechanisms and there is a fine balance between the two which, when perturbed, can have dramatic effects on the regulation of AJs.

Introduction

In their physiological environment, cells are in contact with neighboring cells. Cadherin-based AJs provide the initial means of cell-cell contact and have key roles during development and maintenance of epithelial polarity.[1,2] Additionally, there is overwhelming evidence that the AJ is an important tumor and/or invasion suppressor.[3-5] E-cadherin, the prototypic classical cadherin, is ubiquitously expressed in epithelial tissues. In common with other classical cadherins, E-cadherin is a single pass transmembrane protein with an extracellular domain consisting of five extracellular repeats that mediate either calcium-dependent homotypic interactions with the cadherin molecules of an adjacent cell[6] or with cadherins in the same membrane.[7]

AJs are not static but rather must be amenable to rapid remodeling, for example during embryogenesis or wound healing. The ability of E-cadherin molecules to respond to external stimuli is key to controlling the formation and turnover of AJs and the highly dynamic nature of E-cadherin molecules within the membrane makes this possible.[8,9] E-cadherin is present in two pools within the membrane: diffusible E-cadherin molecules and transmembrane clusters engaged in cell-cell adhesion, and the movement of E-cadherin molecules between these two pools governs the formation of stable junctions.[8,10-12] The concentration of E-cadherin molecules at the membrane is also controlled by endocytosis which in turn can control E-cadherin clustering and junction formation.[13,14] The mechanisms that regulate the movement of E-cadherin within and away from the membrane are not fully understood. Recent studies using FRAP of GFP-E-cadherin have provided information on how the movement of E-cadherin molecules within the membrane are controlled.[9,15,16] However, using FRAP alone, it is not possible to determine the relative importance of endocytosis and lateral movement within the membrane to overall E-cadherin dynamics. To address this we have used photoactivatable green fluorescence protein (PAGFP) fused to E-cadherin, which allows us to follow both the fate and dynamics of E-cadherin molecules following photoactivation. Specifically we wished to look at E-cadherin dynamics in mature junctions as the maintenance of steady state kinetics is critical to the ability of epithelial cells to remodel AJs in response to external stimuli. Therefore, confluent monolayers of A431 squamous cell carcinoma cells were used in this study and we show that the use of photoactivation and photobleaching allows the dynamic regulation of E-cadherin to be followed which is not possible using conventional technologies in fixed sections.

Results

Generation of A431 PAGFP-E-cadherin cell line. In order to carry out photoactivation studies, we stably expressed PAGFP-E-cadherin in A431 cells and we compared its levels of

*Correspondence to: Marta Canel; Email: m.canel@ed.ac.uk
Submitted: 03/30/10; Accepted: 06/15/10
Previously published online: www.landesbioscience.com/journals/celladhesion/article/12661
DOI: 10.4161/cam.4.4.12661

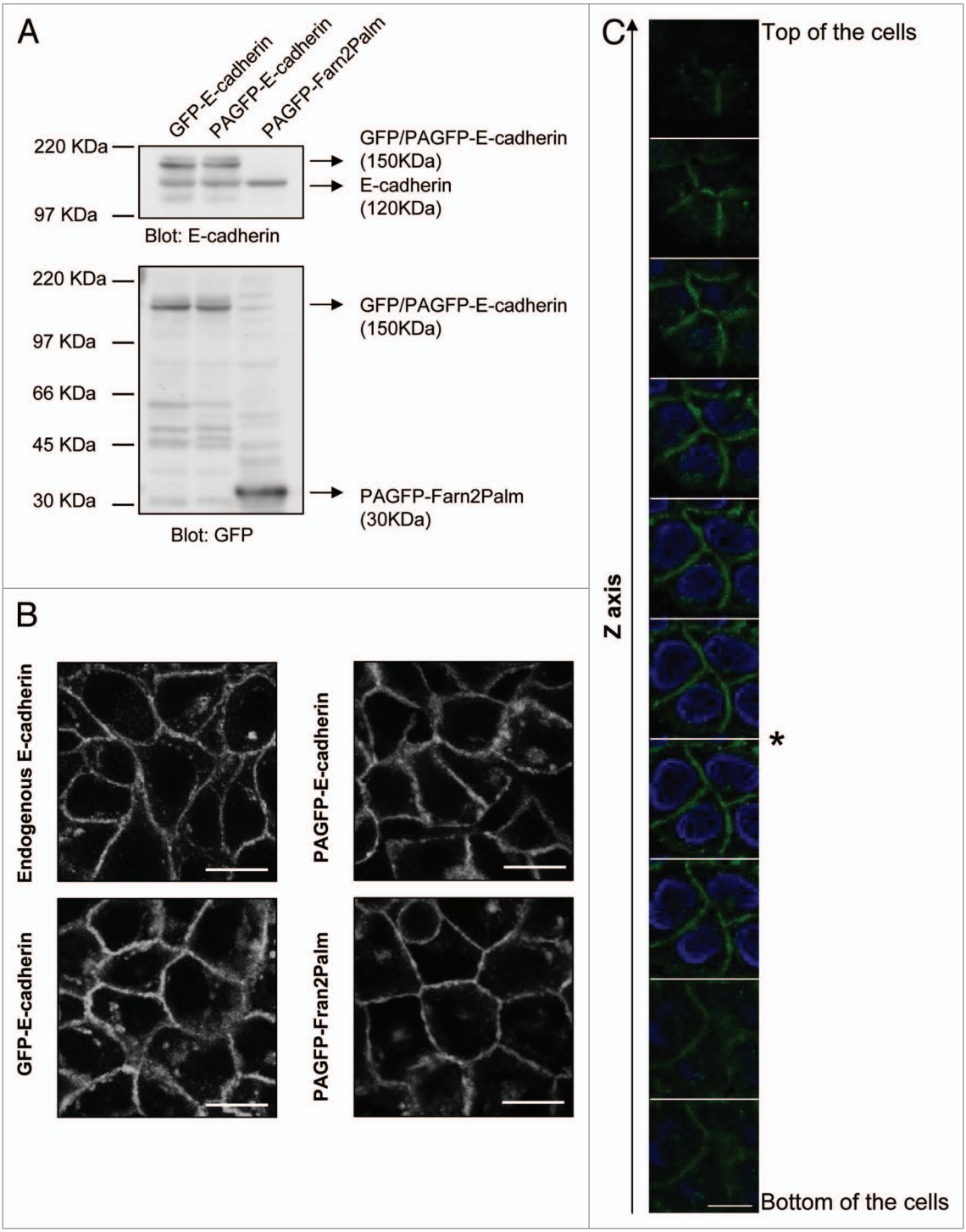

Figure 1. Characterization of A431 cells expressing GFP-E-cadherin, PAGFP-E-cadherin and PAGFP-Farn2Palm. Expression and cellular localization of GFP-E-cadherin, PAGFP-E-cadherin and PAGFP-Farn2Palm in stable pools of A431 were confirmed by immunoblot of E-cadherin and GFP (A) and immunofluorescence of GFP (B). (C) Montage showing cellular localization of GFP-E-cadherin at different levels in the z-axis of the cells. The asterisk (*) indicates the focal plane chosen for E-cadherin dynamics analyses. Blue, DAPI staining. Scale bars, 20 μm.

expression and localization with those of a previously reported A431 GFP-E-cadherin cell line.[17] **Figure 1A** shows similar levels of both endogenous and fluorescence-tagged E-cadherin in these two cell lines detected using both anti-E-cadherin and anti-GFP antibodies. We also generated A431 cells expressing PAGFP-Farn2Palm, where the PAGFP is anchored to the plasma membrane through a farnesylated and doubly palmitoylated membrane targeting sequence.[17,18] Use of PAGFP-Farn2Palm allows us to compare PAGFP-E-cadherin dynamics with that of a probe that diffuses freely within the plasma membrane

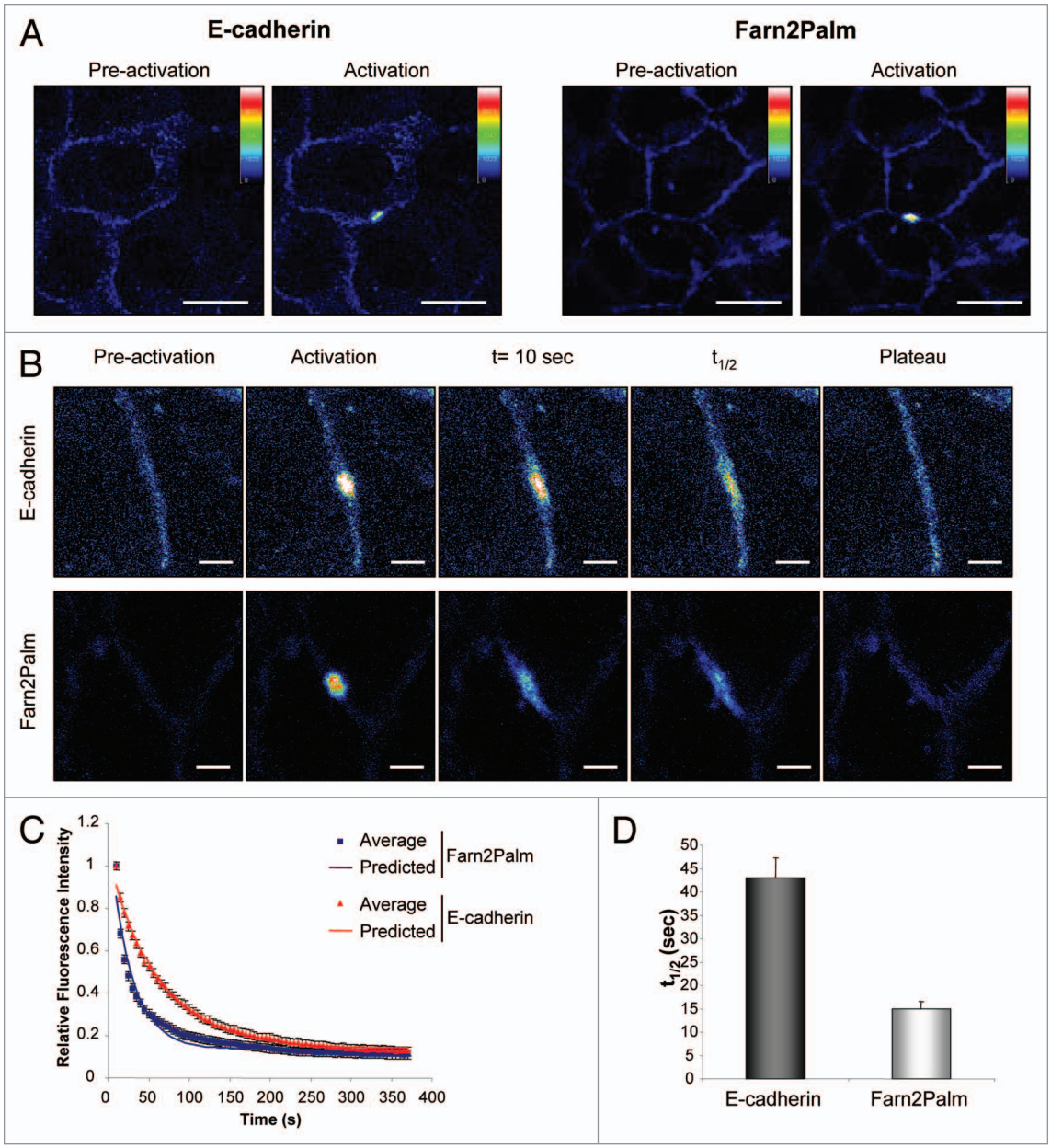

Figure 2. Study of E-cadherin dynamics using photoactivation. (A) Representative images captured pre-activation and following activation showing basal fluorescence of PAGFP-E-cadherin and PAGFP-Farn2Palm when illuminated with 488 laser. Fluorescence intensity heat maps have been applied to facilitate visualization. Scale bars, 20 μm. (B) Representative still images of PAGFP-E-cadherin (top parts) and PAGFP-Farn2Palm (bottom parts) at the plasma membrane captured pre-activation and following activation. Fluorescence intensity heat maps have been applied to facilitate visualization. Scale bars, 5 μm. (C) Fluorescence decay curves following photoactivation of PAGFP-E-cadherin (red) and PAGFP-Farn2Palm (blue). (D) Quantification of $t_{1/2}$ following photoactivation of PAGFP-E-cadherin and PAGFP-Farn2Palm. Values represent the mean from at least 25 cells. Error bars, s.e.m.

and is not specifically removed by endocytosis. Expression of PAGFP-Farn2Palm was confirmed by immunodetection using an anti-GFP antibody (**Fig. 1A**). GFP-E-cadherin and PAGFP-E-cadherin were predominantly located at the plasma membrane in confluent monolayers of A431 cells and showed a similar localization as endogenous E-cadherin (**Fig. 1B**). The localization of GFP-E-cadherin was observed to be more diffuse at the bottom and top of cell, becoming more enriched at sites of AJs (**Fig. 1C**). E-cadherin dynamics were monitored at this level. PAGFP-Farn2Palm was also located at the plasma membrane (**Fig. 1B**).

Characterization of E-cadherin dynamics using photoactivation. Initially we looked at the fate of PAGFP-E-cadherin molecules following photoactivation. Both PAGFP-E-cadherin and PAGFP-Farn2Palm displayed low level of basal fluorescence when illuminated with the 488 laser used for imaging. This basal fluorescence was used to identify a target region in the plasma membrane to photoactivate (**Fig. 2A**). Photoactivation occurred within the next frame acquired following activation (**Fig. 2A**), resulting in a 7.7 ± 0.6 or a 14.3 ± 0.8 fold increase of fluorescence intensity of PAGFP-E-cadherin or PAGFP-Farn2Palm,

respectively. Lateral movement of PAGFP-E-cadherin within the membrane following photoactivation was seen but there was no visual evidence that the probe was internalized (**Fig. 2B**, top parts). A similar lateral movement within the membrane was seen following photoactivation of the membrane targeted PAGFP, PAGFP-Farn2Palm, which is not specifically removed by endocytosis (**Fig. 2B**, bottom parts). Visual comparison of still images acquired 10 seconds after photoactivation clearly indicated that E-cadherin movement within the membrane was much slower than that of the membrane probe. This observation was confirmed by calculation of the half time of recovery ($t_{1/2}$) after fitting of decay curves in SigmaPlot (**Fig. 2C**) (PAGFP-E-cadherin: 43 ± 4 sec; PAGFP-Farn2Palm: 15 ± 2 sec) (**Fig. 2D**). To make sure that the fluorescence decay observed following activation was not caused by photobleaching of the sample during imaging, A431 cells expressing PAGFP-E-cadherin were fixed and photoactivation was carried out as previously. No fluorescence decay was monitored in the time frame of our experiments (data not shown).

In addition, the use of photoactivation allowed further analysis of E-cadherin movement within the membrane; Gaussian curves were obtained by fitting integrated intensity measurements derived from line profiles for both probes at activation and $t_{1/2}$ time points. These curves graphically depict the style of movement within the membrane (**Fig. 3A**) and given the tight fit of our data with R^2 values ranging from 0.93 to 0.98, they clearly show that the predominant mode of E-cadherin movement is laterally within the membrane. Using these Gaussian curves we were also able to calculate the speed of the lateral movement (E-cadherin: 25 ± 0.8 nm/sec; Farn2Palm: 251 ± 4.8 nm/sec) (**Fig. 3B**), again confirming that E-cadherin movement within the membrane is significantly slower than the membrane probe.

E-cadherin is mainly retained at the plasma membrane of confluent monolayers of A431 cells. Using the photoactivatable probes also allows us to quantify the fraction of fluorescent molecules retained in the membrane following photoactivation. We measured the initial integrated intensity of the activated region and the intensity of the thresholded segmented region at the $t_{1/2}$ for both probes. Examples of the still images from photoactivation experiments and corresponding segmented regions which were analyzed in ImageJ to obtain these measurements are shown in **Figure 4A**. In the case of the membrane targeted PAGFP-Farn2Palm, 80 ± 2.3% of the fluorescence signal was retained in the membrane region. This value is most likely an underestimate of the fraction retained within the membrane as the technique was not sensitive enough to quantify the fluorescence signal as it reached background levels at the edge of the spread photoactivated region. In addition, all images were recorded in a single focal plane, which is inevitably subject to loss of fluorescence signal via 3-dimensional movement of the photoactivated probe within the membrane. However, the fraction of PAGFP-E-cadherin signal retained over its $t_{1/2}$ was significantly smaller than the membrane probe (69 ± 2.2%; t test, p = 0.003) (**Fig. 4B**), which allowed us to infer that a relatively small but significant fraction (around 10%) of E-cadherin molecules may be lost from the plasma membrane.

As around 90% of the E-cadherin molecules remain within the membrane in the time frame of these experiments, we propose that the E-cadherin dynamics quantified by FRAP are likely to be a reflection of the lateral movement of E-cadherin molecules within the membrane. In agreement with the results obtained from the photoactivation analysis we found that GFP-E-cadherin moved more slowly than GFP-Farn2Palm ($t_{1/2}$ for GFP-E-cadherin was 85 ± 6 sec compared to 15 ± 1 sec for GFP-Farn2Palm following photobleaching) (**Fig. 5C**). These results were also supported by analyses of the type of movement of these probes following photobleaching. Similar to described above, integrated intensity measurements derived from line profiles for both probes at bleaching and $t_{1/2}$ time points were fitted to gaussian curves (R^2 = 0.92–0.99) (**Fig. 3C**) and used to calculate the speed of the lateral movement (E-cadherin: 6.6 ± 0.5 nm/sec; Farn2Palm: 17.8 ± 1.5 nm/sec) (**Fig. 3D**), again confirming that E-cadherin movement within the membrane is significantly slower than the membrane probe.

Deregulation of exchange between the intracellular pool of E-cadherin and the cell surface specifically alters the rate of movement of E-cadherin at the plasma membrane. Photoactivation data suggested that active withdrawal of E-cadherin molecules from the plasma membrane could be occurring in confluent monolayers of A431 cells. To confirm this, we carried out biochemical analyses, which showed that surface biotinylated E-cadherin was internalized in the time frame of our experiments (**Fig. 5A**). Densitometric quantification revealed that the proportion of surface E-cadherin internalized over a period of 10 min was around 15%, in agreement with results obtained in our PA analyses. In addition, we observed that both endogenous and exogenous E-cadherin pools were similarly internalized, indicating that the fluorescence tag did not disrupt E-cadherin regulation (data not shown). To determine whether intracellular trafficking could affect the lateral movement of E-cadherin we made use of pharmacological agents that block this process at different levels. Firstly, we used dynasore, a potent dynamin inhibitor that blocks vesicles pinching off the membrane.[19] Dynasore impaired E-cadherin internalization, as shown in a cell surface biotinylation assay (**Fig. 5A**). In order to study the impact on E-cadherin dynamics, we carried out FRAP experiments and calculated the $t_{1/2}$ derived from the recovery curves of each probe (**Fig. 5B**). As expected, the $t_{1/2}$ of the membrane probe remained unchanged upon treatment of cells with dynasore as it is not specifically endocytosed (**Fig. 5C**). In contrast, E-cadherin molecules moved significantly faster after blocking endocytosis with dynasore (**Fig. 5C**). Secondly, we used the potent ATPase inhibitor, bafilomycin A1.[20] Biotinylation assays revealed that bafilomycin A1 increased the E-cadherin intracellular pool, likely as a consequence of this drug's effects on derailing the recycling from intracellular pools back to the membrane (**Fig. 5A**). As with dynasore, treatment with bafilomycin A1 decreased the $t_{1/2}$ after photobleaching of GFP-E-cadherin (**Fig. 5C**). In addition, following photoactivation of PAGFP-E-cadherin, line profile analyses of cells treated with bafilomycin A1 revealed an increased rate of motility of E-cadherin molecules within the membrane (**Fig. 5D**).

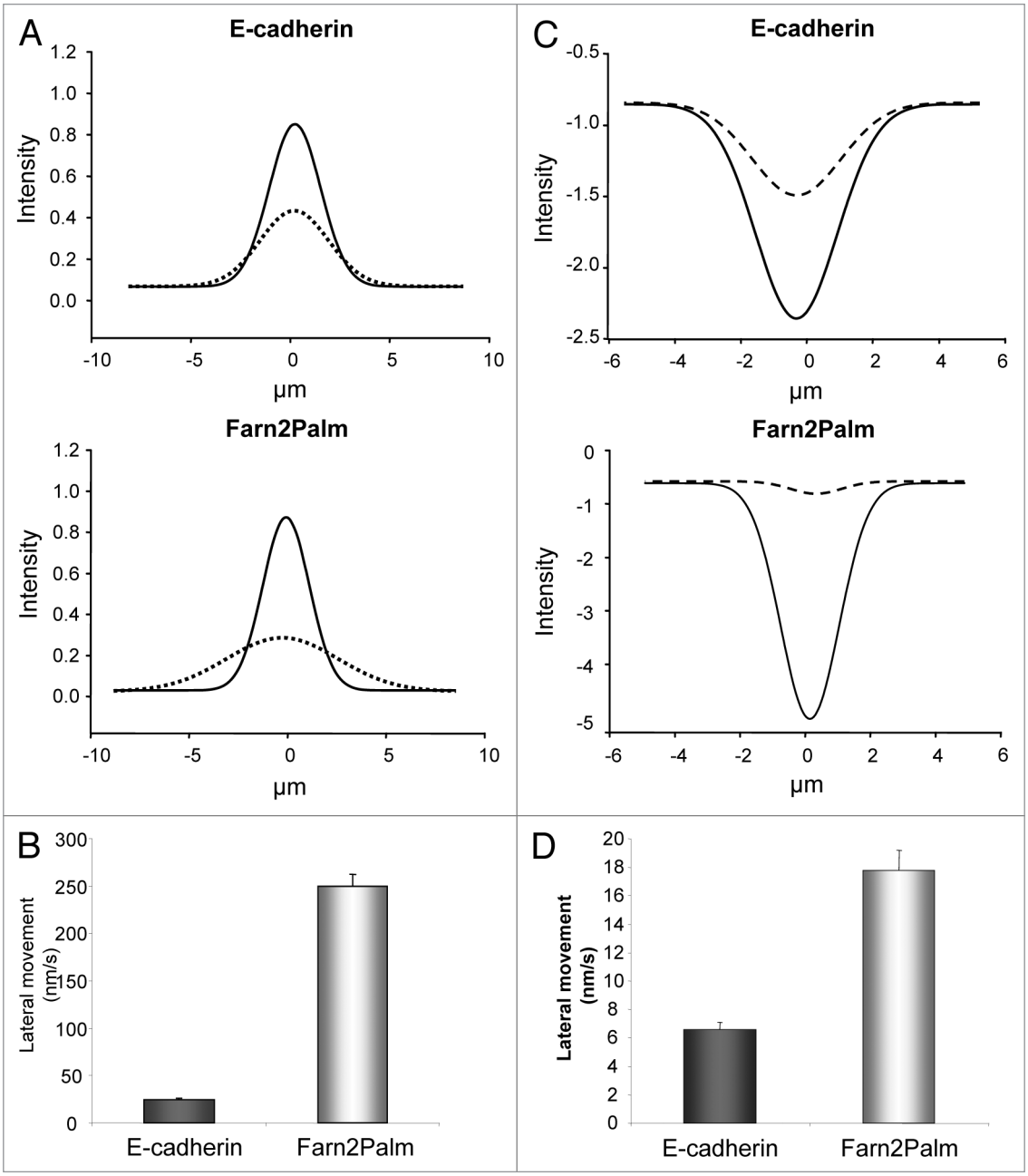

Figure 3. Monitoring E-cadherin dynamics at the plasma membrane. (A) Integrated fluorescence intensity measurements over the plasma membrane at activation (full line) and $t_{1/2}$ time points (dash line) were fitted to Gaussian curves for PAGFP-E-cadherin (top) and PAGFP-Farn2Palm (bottom). (B) Quantification of the speed of lateral movement of PAGFP-E-cadherin and PAGFP-Farn2Palm within the membrane. (C) Integrated fluorescence intensity measurements over the plasma membrane at bleaching (full line) and $t_{1/2}$ time points (dash line) were fitted to Gaussian curves for GFP-E-cadherin (top) and GFP-Farn2Palm (bottom). (D) Quantification of the speed of lateral movement of GFP-E-cadherin and GFP-Farn2Palm within the membrane. Values represent the mean from at least 25 cells. Error bars, s.e.m.

E-cadherin immobile fraction is not perturbed by inhibiting intracellular trafficking. As reported in our previous study,[17] the fluorescence intensity of GFP-E-cadherin in the plasma membrane after photobleaching never recovers to the original value. This is attributed to a fraction of E-cadherin molecules that are unable to move (termed immobile fraction). The immobile fraction of GFP-E-cadherin was significantly higher than GFP-Farn2Palm (20 ± 2% and 10 ± 1%, respectively) (**Fig. 6**), which is in agreement with the PA data, indicating that E-cadherin is less freely diffusible within the membrane than the Farn2Palm probe. Dynasore treatment did not affect the immobile fraction of GFP-Farn2Palm and, interestingly, the E-cadherin immobile fraction also remained unchanged in the presence of dynasore and bafilomycin A1 (**Fig. 6**), suggesting that changes in intracellular trafficking does not alter the proportion of E-cadherin molecules at the membrane which are able to move.

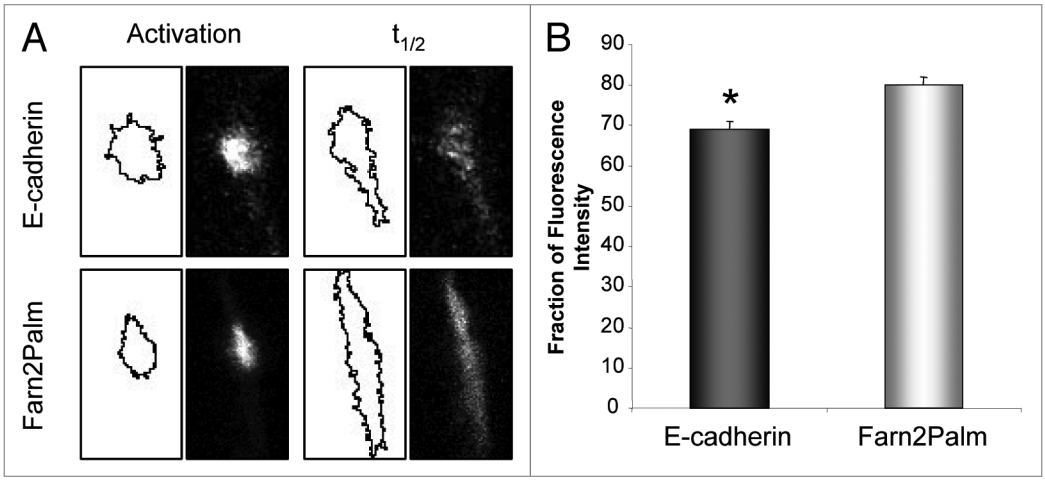

Figure 4. E-cadherin is mainly retained at the plasma membrane of confluent monolayers of A431 cells. (A) Segmentation of fluorescence signal using ImageJ and corresponding still images from photoactivation experiments at activation and $t_{1/2}$ time points for PAGFP-E-cadherin and PAGFP-Farn2Palm used for membrane retention analyses. (B) Quantification of the proportion of fluorescence intensity that is retained in the plasma membrane at $t_{1/2}$ following activation of PAGFP-E-cadherin and PAGFP-Farn2Palm. (t test, *p = 0.003). Values represent the mean from at least 25 cells. Error bars, s.e.m.

Inhibition of endocytosis strengthens cell-cell adhesion. Intracellular trafficking was found to play a crucial role in controlling the rate of movement of the E-cadherin molecules within the membrane. This therefore raises the question of whether the endocytosis of E-cadherin molecules is physiologically important and can affect cell-cell adhesion strength. To measure adhesion strength, confluent monolayers of cells were incubated with dispase. This results in detachment of the cells as an intact monolayer. The resistance to disaggregation induced by mechanical stress of these monolayers is then used as a measure of the relative strength of cell-cell contacts. Treatment with dynasore resulted in an increased size of the fragments released (**Fig. 7A**) and a reduction in the number of single cells detached from the cell sheets (**Fig. 7B**). This result indicated a strengthening effect of dynasore on cell-cell adhesion. As expected, changes in E-cadherin expression levels had an impact on cell-cell junction strength measure by dispase assay. Overexpression of E-cadherin resulted in a reduction in the number of single cells detached from the cell sheets, while inhibition of E-cadherin expression by siRNA decreased adhesion strength (**Fig. 7C**). These results support the use of this assay as a readout of the ability of A431 cells to establish and maintain E-cadherin-dependent cell-cell adhesions. However, inhibition of endocytosis following treatment of cells with dynasore did not change the levels of E-cadherin at the membrane as visualized at the time of FRAP acquisition or result in the loss of AJ integrity (**Fig. 7D**). In order to detect any potential changes in levels of E-cadherin in the cell surface upon in A431 cells treated with dynasore, we incubated cells with biotin at 4°C to prevent internalization and surface E-cadherin molecules were collected with Agarose Immobilized Streptavidin. Proteins were eluted by boiling the beads in SDS sample buffer and analyzed by SDS-PAGE and immunoblotting with an anti-E-cadherin antibody. Alternatively, total protein lysates were resolved in parallel and probed for total E-cadherin expression. No detectable changes were identified in surface or total levels of E-cadherin (**Fig. 7E**). These observations support the data presented above, indicating that only a small proportion of E-cadherin molecules are subject to endocytosis in confluent monolayers of A431 cells. Furthermore, disrupting the endocytic machinery can have significant effects on cell-cell adhesion strength.

Discussion

The dynamic remodeling of E-cadherin-mediated AJs at the plasma membrane is crucial for epithelial homeostasis and its deregulation has been involved in several diseases, including cancer.[3-5] Several studies have now suggested different mechanisms that regulate E-cadherin dynamics at the plasma membrane, albeit their interplay and contribution to E-cadherin function is not fully understood. Here we have used photoactivation and FRAP to monitor the fate of E-cadherin molecules within the cell. The movement of PAGFP-E-cadherin was analyzed in comparison to a photoactivatable membrane targeted GFP (PAGFP-Farn2Palm). The freely diffusing PAGFP-Farn2Palm was observed to undergo rapid lateral diffusion. Similarly, photoactivation of PAGFP-E-cadherin revealed that it also underwent lateral movement within the plasma membrane, however with a slower rate of movement. Fitting of data derived from line profile analysis to Gaussian curves confirmed that the predominant mode of movement for both probes was lateral along the membrane, and that the movement of PAGFP-Farn2Palm was up to ten times faster than that of E-cadherin. These results are consistent with a model suggesting that the majority of E-cadherin molecules are not freely diffusible within the membrane, but rather their movement is restricted either through cadherin clustering at AJs or via tethering to the microtubule network or actin cytoskeleton.[9,12,16,21]

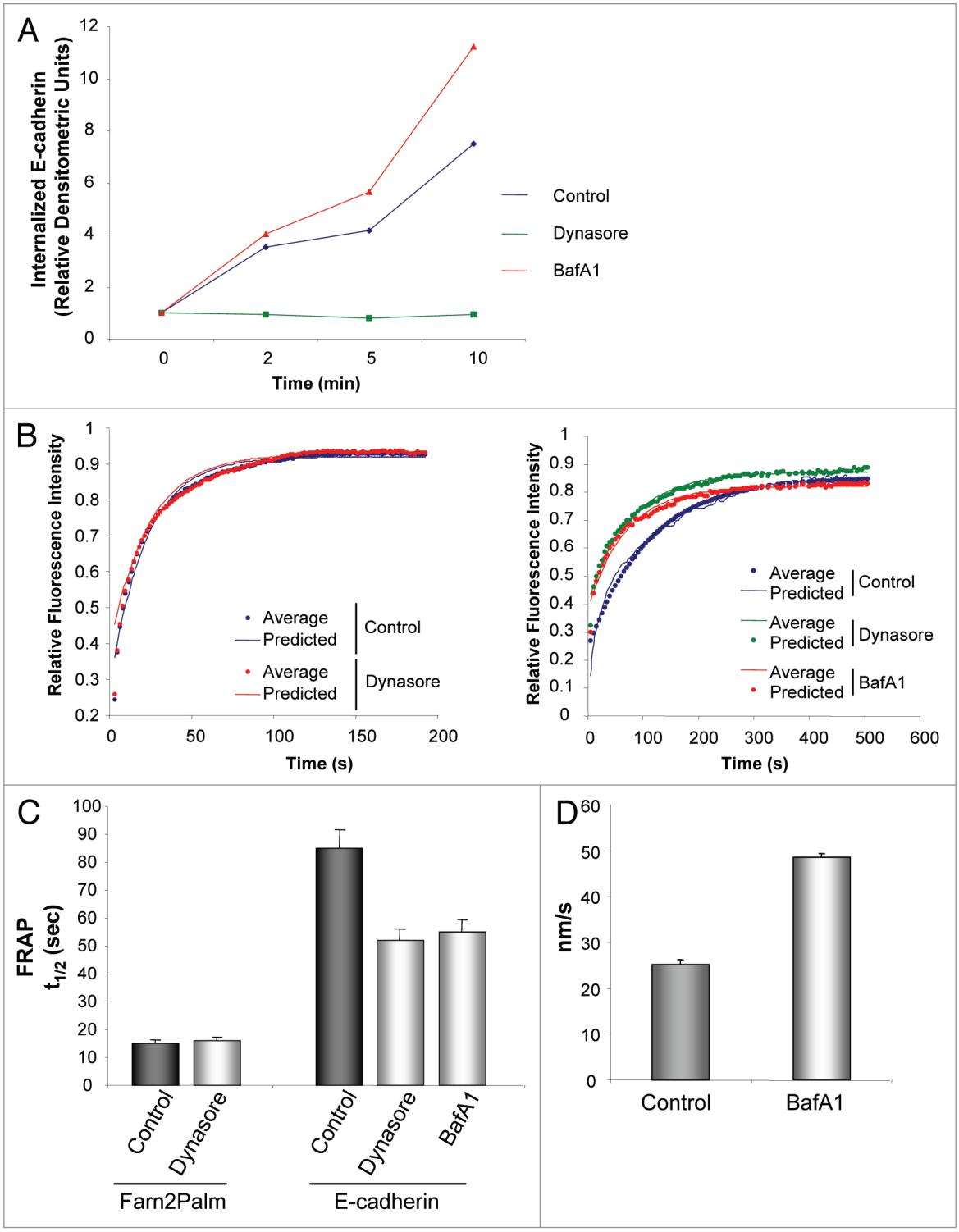

Figure 5. Deregulation of intracellular trafficking specifically alters the rate of movement of E-cadherin at the plasma membrane. (A) Quantification of biotinylated E-cadherin internalization over 10 min in A431 cells or A431 cells treated with either dynasore or bafilomycin A1 (dynasore 80 μM, bafilomycin A1 1 μM, 30 min). (B) Fluorescence recovery curves following photobleaching of GFP-Farn2Palm (left part) and GFP-E-cadherin (right part) in control cells (blue) or cells treated with dynasore (red) or bafilomycin A1 (green), (dynasore 80 μM, bafilomycin A1 1 μM, 0.5–2 h). (C) Quantification of $t_{1/2}$ following photobleaching of GFP-Farn2Palm in control or dynasore-treated cells or GFP-E-cadherin in control cells or cells treated with either dynasore or bafilomycin A1. (D) Quantification of the speed of lateral movement of PAGFP-E-cadherin within the membrane in cells treated with bafilomycin A1. Values represent the mean from at least 25 cells. Error bars, s.e.m.

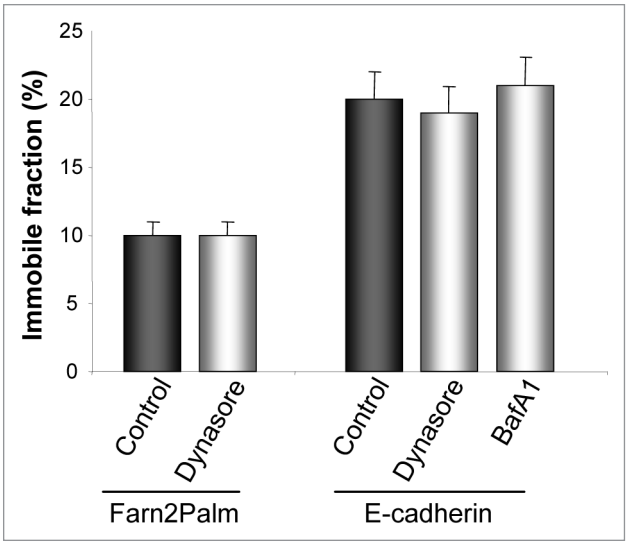

Figure 6. The immobile fraction of E-cadherin at the plasma membrane is not perturbed by dynasore or bafilomycinA1. Quantification of immobile fraction following photobleaching of GFP-Farn2Palm in control or dynasore-treated cells or GFP-E-cadherin in control cells or cells treated with either dynasore or bafilomycin A1 (dynasore 80 μM, bafilomycin A1 1 μM, 0.5–2 h). Values represent the mean from at least 25 cells. Error bars, s.e.m.

E-cadherin is reported to undergo both diffusion within the membrane[22] and active withdrawal from and recycling back to the membrane via intracellular trafficking networks.[13,23] Reports in confluent monolayers of other epithelial cells have shown that only a small pool of around 10–15% of E-cadherin molecules are constantly cycled through an endocytic pathway.[13,24] Despite the limitations imposed by the use of confocal microscopy that we described above, our photoactivation results are in agreement with these reports. In addition, our imaging approaches were supported by the results obtained in the biochemical analyses. Taken together, we suggest that in A431 confluent monolayers the majority of E-cadherin molecules are highly dynamic within the membrane but there is still a small proportion that is subject to endocytosis.

These findings suggest that E-cadherin dynamics might be simultaneously governed by lateral movement and endocytosis, and what could be pivotal in its regulation would be a tight balance of these two contributing factors. To assess our hypothesis, we utilized two broadly used drugs, dynasore and bafilomycin A1, which impair trafficking from and to the plasma membrane, respectively, and we carried out photoactivation and photobleaching studies. These results revealed that the rate of lateral movement of E-cadherin at the membrane was increased as a consequence of inhibiting its intracellular trafficking. This may reflect a change in the dynamic interplay between adhesive E-cadherin molecules associated with cell-cell interactions and the lateral movement of E-cadherin molecules not engaged in adhesions, as endocytosis has been shown to target both of these pools of E-cadherin.[14,25] These results indicate that the endocytic and recycling machinery contribute to the maintenance of E-cadherin dynamics found at a steady state in mature AJs. Although the majority of E-cadherin molecules are retained within the membrane of mature junctions, disruption of the endocytic and recycling pathways has significant effects on the movement of E-cadherin within the membrane.

It therefore seems reasonable to propose that an intimate relationship between E-cadherin endocytosis and lateral membrane diffusion may exist and that this relationship may be important in determining cell-cell adhesion strength. Indeed, we showed that A431 cells treated with dynasore presented resistance to mechanical dissagregation of a cellular sheet. These results strongly indicate a relationship between the inhibition of E-cadherin endocytosis and cell-cell adhesion strength. However, there might be other levels of regulation that could be taking place simultaneously. For instance, intracellular pools of E-cadherin and other AJs components have been shown to be involved in diverse signaling pathways, which in return could affect cell-cell adhesion strength when deregulated.[26] Also, the role of cortical signaling being potentially affected by the drugs used in this study cannot be ruled out.

E-cadherin does not solely exist as freely diffusible monomers within the membrane. It was identified some time ago that E-cadherin molecules can homodimerize or oligomerize to form higher-order complexes known as cadherin "clusters."[27] The parallel orientation of these between cells has been proposed to increase cell-cell adhesion strength[23] and more recently, FRAP analysis of molecular dynamics within these structures has shown them to be relatively immobile. In fact, these clusters are reported to be extremely stable and undergo very little exchange of their molecular contents with the freely diffusing E-cadherin pool at the membrane.[9] Recently Cavey and colleagues reported these structures as "bona fide sites of adhesion;" yet, following targeted downregulation of the cadherin/catenin/actin-associated protein α-catenin, cell-cell adhesions were noted to collapse without the dissociation and loss of cadherin clusters. No investigation was reported into the fate of the mobile E-cadherin pool following collapse of these adhesions. In our hands, no change was detected in the E-cadherin immobile component upon strengthening of cell-cell adhesion, suggesting that immobilized E-cadherin may not be the fundamental component involved in this process. In support of this notion, experiments utilizing laser trapping of E-cadherin-coated beads suggested that the initial accumulation of E-cadherin at sites of cell-bead interaction was dependent on active membrane dynamics, and relied on the diffusion mediated trapping of E-cadherin molecules at these sites.[22] In light of these results, we suggest here that AJs could be susceptible to continuous turnover, and the regulation of the interchange between E-cadherin molecules involved and not involved in adhesive complexes might determine the strength and ability to remodel cell-cell adhesions. Further investigation will be required to elucidate the role of E-cadherin clusters in cell-cell adhesion and the dynamics of their formation and remodeling.

In conclusion, we have provided novel insights into the mechanisms regulating E-cadherin dynamics. Currently there are two models to explain the control of E-cadherin localization to AJs, one based on the lateral movement of E-cadherin within the membrane to sites of adhesion and the other on endocytosis. Here

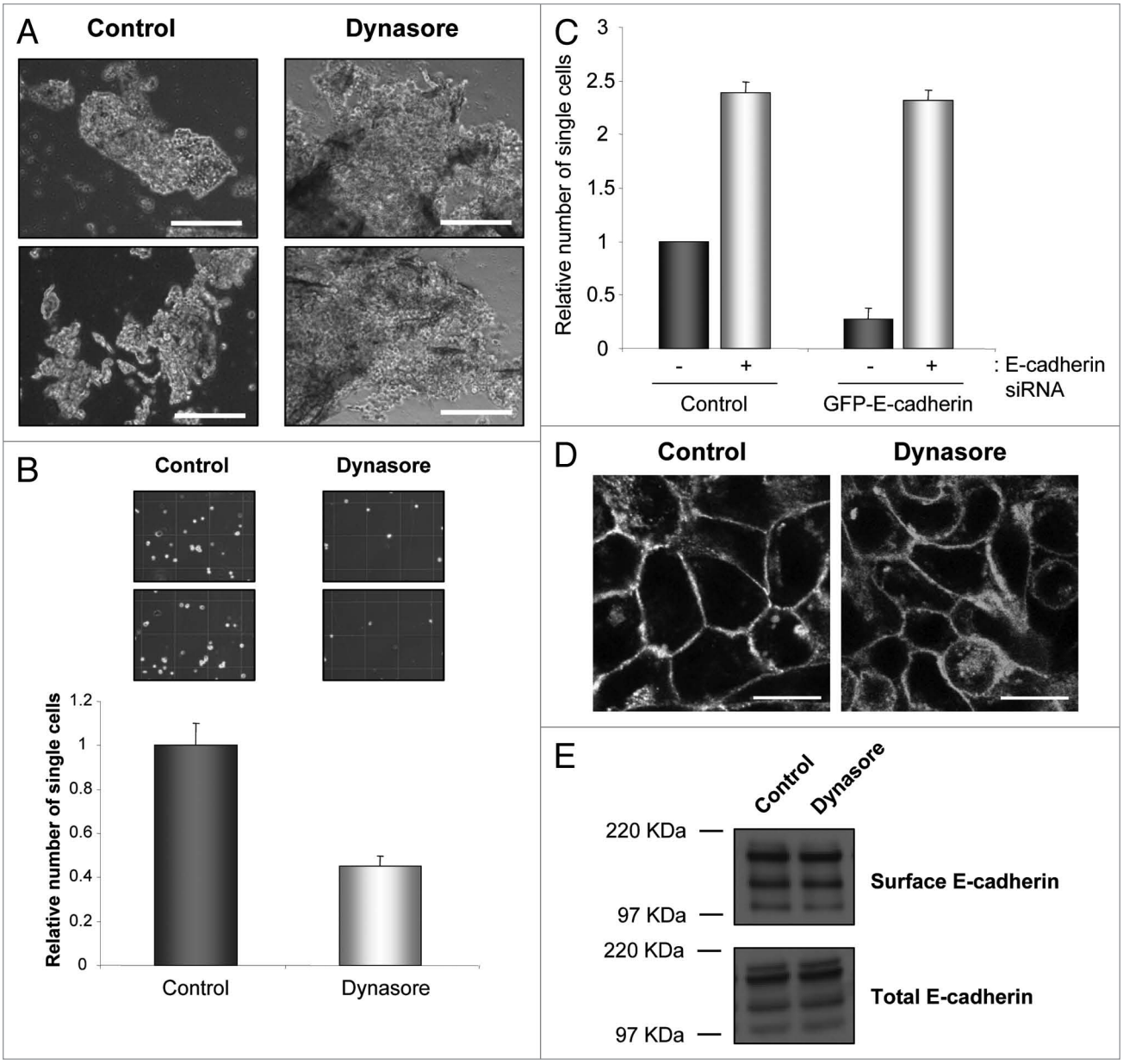

Figure 7. Inhibition of endocytosis strengthens cell-cell adhesion. (A) Representative images of fragments detached from a dispase-treated monolayer of control or dynasore (80 μM, 30 min) pre-treated A431 cells after mechanical stress. (B) Quantification of the number of single cells that disaggregate from a dispase-treated monolayer after mechanical stress. (C) Quantification of the number of single cells that disaggregate after mechanical stress from a dispase-treated monolayer of A431 or A431 GFP-E-cadherin cells, transfected with either control or E-cadherin siRNA. (D) Still images obtained from photobleaching experiments showing GFP-E-cadherin localization in A431 cells untreated or treated with dynasore (80 μM, 30 min). Scale bars, 20 μm. (E) Immunoblot showing surface and total levels of GFP- and endogenous E-cadherin (150 kDa and 120 kDa, respectively) in A431 cells untreated or treated with dynasore (80 μM, 30 min). (B and C) Values represent the mean from at least three independent experiments. Error bars, s.e.m.

we propose that these two mechanisms are not exclusive or independent and that there is a fine balance between the two which when perturbed can have dramatic effects on the regulation of AJs. Importantly these changes in E-cadherin dynamics occur without any visible changes in E-cadherin localization at the membrane or adhesion integrity and highlight the requirement to use technologies like PA and FRAP to look in close detail at the dynamic regulation of E-cadherin. The ability to use these techniques in live animals has opened up the possibility of using E-cadherin dynamics as a molecular read-out of the early mobilization events in tumor cells and the subsequent testing of potential anti-invasive agents.[17]

Materials and Methods

Constructs. GFP-E-cadherin in pcDNA3 was a kind gift from Jennifer Stow.[28] Photoactivatable GFP (PAGFP) in the pEGFP-N1 vector backbone was kindly provided by Jennifer Lippincott-Schwartz.[29] PAGFP-E-cadherin was made by replacing GFP from the original GFP-E-cadherin construct with PAGFP using the SacII and Xba1 restriction sites. The sequence of PAGFP-E-cadherin was confirmed by sequencing with T7 and SP6 primers. The cloning strategies to develop GFP/PAGFP-Farn2Palm were described previously.[17,18,30]

Cell culture. A431 skin epidermoid carcinoma cells were obtained from the American Type Tissue Collection (LGC Promochem) and cultured in DMEM (Invitrogen) supplemented with 10% fetal bovine serum and 2 mM L-glutamine (Invitrogen). A431 cells were transfected with 5 μg of GFP- or PAGFP-E-cadherin/Farn2Palm using the Amaxa nucleofector transfection system with solution V and electroporation program P20 (Amaxa GmbH) as detailed in the manufacturers protocol. Transfected cells were allowed to recover for 24 h and then cells positive for GFP expression were selected using 0.6 mg/ml G418. Single cell clones were isolated from stably expressing selected pools using a standard dilution cloning procedure. The following treatments were used in this study: dynasore (Sigma) 80 μM, bafilomycin A1 (Sigma) 1 μM all for 0.5–2 h.

Cell surface biotinylation assay for endocytosis. Quantification of the endocytosis of biotinylated protein was performed according to a previously published method.[13] Briefly, A431 cells were incubated with 0.2 mg/ml sulfosuccinimidyl 2-(biotinamido) ethyl-dithioproprionate (Pierce) at 4°C for 30 min. Cells were washed with PBS and surface E-cadherin detected by immunoprecipitation with Streptavidin as described below. Alternatively, after biotinylation, cells were then cultured in growth media at 37°C to allow internalization of biotinylated E-cadherin. At the indicated times the remaining cell surface biotin groups were removed by washing the cells twice in a solution containing 50 mM Tris-HCl pH 8.6, 100 mM NaCl, 2.5 mM $CaCl_2$ and 50 mM 2-mercaptoethanesulfonate at 4°C for 20 min. The cells were then washed with PBS and lysed in RIPA buffer containing 20 mM Tris-HCl, pH 7.4, 150 mM NaCl, 1% (v/v) Triton X-100, 0.1% (w/v) SDS, 1% (w/v) deoxycholate, 5 mM EDTA and protease inhibitors. Internalized biotinylated proteins were collected with Agarose Immobilized Streptavidin (Sigma). Proteins were eluted by boiling the beads in SDS sample buffer and analyzed by SDS-PAGE and immunoblotting with an anti-E-cadherin antibody as described below. Densitometry analysis was carried out using ImageJ software and the results presented as fold change in internalized E-cadherin over time compared to the non-internalized level at 0 h. Results are shown from a representative experiment in a series of at least three.

Immunoblot analysis. Immunoblot analysis was performed as previously described.[31] Primary antibodies used were anti-E-cadherin, (Becton Dickinson Transduction Laboratories) and anti-GFP (Abcam) all at 1:1,000 dilution.

Confocal immunofluorescence microscopy. A431 cells were fixed and permeabilized with buffer containing 100 mM PIPES, 10 mM EGTA, 1 mM MgCl2, 0.2% (v/v) Triton-X-100, 3.7% (v/v) formaldehyde for 15 min and blocked with 5% (v/v) fetal bovine serum, 2% (w/v) BSA, 0.1% (v/v) Triton-X-100 in TBS for an 1 h. Primary antibody used was anti-GFP (Abcam) at 1:100 dilution. Cells were washed and incubated with AlexaFluor488-conjugated anti-rabbit IgG antibody (Molecular Probes) and examined using an Olympus FV1000 confocal microscope.

Dispase-based dissociation assay. The assay for measuring cell-cell adhesive strength[32-34] was modified as follows: confluent monolayers of cells were set up in triplicate, washed twice in phosphate-buffered saline and incubated in 1 ml of dispase II (3 mg/ml, 2.4 U/ml; Roche) for 1 h. To apply a mechanical stress, the released monolayers were pipetted 10 times with an automatic pipette and filtered through 40 μm cell strainers. Released single cells were counted in a 10 μl aliquot. One well of each triplicate was treated with trypsin instead of dispase, to determine the total cell number. The number of single cells was then expressed as a percentage of the total cell number in at least three independent experiments.

FRAP and photoactivation analysis. 1.5 x 10^6 cells were plated onto glass-bottomed 30 mm tissue culture dishes (Iwaki Cell Biology) and left to adhere overnight. Culture media was replaced prior to imaging. Photobleaching and activation experiments were performed using an Olympus FV1000 confocal microscope with SIM scanner. Cells were maintained at 37°C in a temperature-controlled chamber and imaging performed using the following settings: pixel dwell time 4 μs/px, pixel resolution 512 x 512, 5% 488 nm laser power (GFP-E-cadherin, GFP- and PAGFP-Farn2Palm) or 70% 488 nm laser power (PAGFP-E-cadherin). Effective photobleaching was achieved using 50% 405 nm laser power, 20 μs/pixel dwell time and a 1 frame bleach time. Images were captured every 5 sec (GFP-E-cadherin) or every 1.6 sec (GFP-Farn2Palm) for 100 frames. Photoactivation was achieved using 5% 405 nm laser power, 4 μs/pixel dwell time (PAGFP-Farn2Palm) or 40 μs/pixel dwell time (PAGFP-E-cadherin) and a 1 frame activation pulse. Images were captured every 5 seconds for 75 frames. Approximately 25 cells were imaged for each probe. Fluorescent intensity measurements derived from the region of interest used to bleach/activate were averaged in Excel and used to plot recovery/decay curves. Average measurements for each time-point were exported into SigmaPlot (Systat Inc.,) for exponential curve fitting. The half-time of recovery ($t_{1/2}$) and immobile fraction were calculated as described previously.[17] Membrane retention analysis was performed using ImageJ software. The images representing the initial activation time-point and $t_{1/2}$ time-point were selected from each time-series, and a standard threshold value applied to all images from the same experiment. The image properties were changed to have a pixel width and height of 1, and the analyze particles function used to calculate the area and mean grey values of the resulting segmented areas within the image. The integrated intensity for the segmented area of interest was calculated by multiplying the area by the mean grey value, and the average remaining florescence

calculated for the $t_{1/2}$ time-point. Lateral movement analysis was performed using ImageJ software. Briefly, cells in which the area of photoactivation was midway along a straight membrane were selected, and a line drawn along this membrane with the point of activation at the centre of the line. A standard threshold value was applied to all images from the same experiment, and fluorescent intensity line-plots generated for each image. Images from the activation time-point and the $t_{1/2}$ time-point were analyzed for each time-series acquired. Line-plot values from these two images were transferred into Excel, normalized to the highest intensity value from the activation time-point, and the multiple datasets aligned using this value as the centre of the Gaussian plot. The aligned normalized values for the two time-points were averaged and fitted to a four parameter Gaussian curve ($y = y_0 + ae[-0.5(x - x_0/b)^2]$) using SigmaPlot. The b parameter was used to calculate the Full Width at Half Maximum of the curves as follows: FWHM = $(2\sqrt{2}\ln 2)b$. The speed of lateral movement was calculated as the difference between FWHM at activation and $t_{1/2}$ points over time.

Acknowledgements

This work was funded by Cancer Research UK Program Grant C157/A9148 and M.C. by Fundación Española para la Ciencia y la Tecnología.

Note

Supplementary materials can be found at:
www.landesbioscience.com/supplement/Canel-CAM4-4-Sup01.mov
Photoactivation of PAGFP-E-cadherin in A431 cells. Images were acquired every 5 seconds.

www.landesbioscience.com/supplement/Canel-CAM4-4-Sup02.mov
Photoactivation of PAGFP-Farn2Palm in A431 cells. Images were acquired every 5 seconds.

References

1. Nelson WJ. Adaptation of core mechanisms to generate cell polarity. Nature 2003; 422:766-74.
2. Thiery JP. Cell adhesion in development: a complex signaling network. Curr Opin Genet Dev 2003; 13:365-71.
3. Hajra KM, Fearon ER. Cadherin and catenin alterations in human cancer. Genes Chromosome Canc 2002; 34:255-68.
4. Nollet F, Berx G, van Roy F. The role of the E-cadherin/catenin adhesion complex in the development and progression of cancer. Mol Cell Biol Res Commun 1999; 2:77-85.
5. Yap AS. The morphogenetic role of cadherin cell adhesion molecules in human cancer: a thematic review. Cancer Invest 1998; 16:252-61.
6. Patel SD, Chen CP, Bahna F, Honig B, Shapiro L. Cadherin-mediated cell-cell adhesion: sticking together as a family. Curr Opin Struct Biol 2003; 13:690-8.
7. Leckband D, Sivasankar S. Mechanism of homophilic cadherin adhesion. Curr Opin Cell Biol 2000; 12: 587-92.
8. Adams CL, Chen YT, Smith SJ, Nelson WJ. Mechanisms of epithelial cell-cell adhesion and cell compaction revealed by high-resolution tracking of E-cadherin-green fluorescent protein. J Cell Biol 1998; 142:1105-19.
9. Cavey M, Rauzi M, Lenne PF, Lecuit T. A two-tiered mechanism for stabilization and immobilization of E-cadherin. Nature 2008; 453:751-6.
10. Brieher WM, Yap AS, Gumbiner BM. Lateral dimerization is required for the homophilic binding activity of C-cadherin. J Cell Biol 1996; 135:487-96.
11. Klingelhofer J, Laur OY, Troyanovsky RB, Troyanovsky SM. Dynamic interplay between adhesive and lateral E-cadherin dimers. Mol Cell Biol 2002; 22:7449-58.
12. Sako Y, Nagafuchi A, Tsukita S, Takeichi M, Kusumi A. Cytoplasmic regulation of the movement of E-cadherin on the free cell surface as studied by optical tweezers and single particle tracking: corralling and tethering by the membrane skeleton. J Cell Biol 1998; 140: 1227-40.
13. Le TL, Yap AS, Stow JL. Recycling of E-cadherin: a potential mechanism for regulating cadherin dynamics. J Cell Biol 1999; 146:219-32.
14. Troyanovsky RB, Sokolov EP, Troyanovsky SM. Endocytosis of cadherin from intracellular junctions is the driving force for cadherin adhesive dimer disassembly. Mol Biol Cell 2006; 17:3484-93.
15. de Beco S, Gueudry C, Amblard F, Coscoy S. Endocytosis is required for E-cadherin redistribution at mature adherens junctions. Proc Natl Acad Sci USA 2009; 106:7010-5.
16. Yamada S, Pokutta S, Drees F, Weis WI, Nelson WJ. Deconstructing the cadherin-catenin-actin complex. Cell 2005; 123:889-901.
17. Serrels A, Timpson P, Canel M, Schwarz JP, Carragher NO, Frame MC, et al. Real-time study of E-cadherin and membrane dynamics in living animals: implications for disease modeling and drug development. Cancer Res 2009; 69:2714-9.
18. Konig I, Schwarz JP, Anderson KI. Fluorescence lifetime imaging: association of cortical actin with a PIP3-rich membrane compartment. Eur J Cell Biol 2008; 87:735-41.
19. Macia E, Ehrlich M, Massol R, Boucrot E, Brunner C, Kirchhausen T. Dynasore, a cell-permeable inhibitor of dynamin. Dev Cell 2006; 10:839-50.
20. Balzac F, Avolio M, Degani S, Kaverina I, Torti M, Silengo L, et al. E-cadherin endocytosis regulates the activity of Rap1: a traffic light GTPase at the crossroads between cadherin and integrin function. J Cell Sci 2005; 118:4765-83.
21. Stehbens SJ, Akhmanova A, Yap AS. Microtubules and cadherins: a neglected partnership. Front Biosci 2009; 14:3159-67.
22. Perez TD, Tamada M, Sheetz MP, Nelson WJ. Immediate-early signaling induced by E-cadherin engagement and adhesion. J Biol Chem 2008; 283:5014-22.
23. Yap AS, Crampton MS, Hardin J. Making and breaking contacts: the cellular biology of cadherin regulation. Curr Opin Cell Biol 2007; 19:508-14.
24. Miyashita Y, Ozawa M. Increased internalization of p120-uncoupled E-cadherin and a requirement for a dileucine motif in the cytoplasmic domain for endocytosis of the protein. J Biol Chem 2007; 282:11540-8.
25. Izumi G, Sakisaka T, Baba T, Tanaka S, Morimoto K, Takai Y. Endocytosis of E-cadherin regulated by Rac and Cdc42 small G proteins through IQGAP1 and actin filaments. J Cell Biol 2004; 166:237-48.
26. Bryant DM, Stow JL. The ins and outs of E-cadherin trafficking. Trends Cell Biol 2004; 14:427-34.
27. Nagar B, Overduin M, Ikura M, Rini JM. Structural basis of calcium-induced E-cadherin rigidification and dimerization. Nature 1996; 380:360-4.
28. Miranda KC, Khromykh T, Christy P, Le TL, Gottardi CJ, Yap AS, et al. A dileucine motif targets E-cadherin to the basolateral cell surface in Madin-Darby canine kidney and LLC-PK1 epithelial cells. J Biol Chem 2001; 276:22565-72.
29. Patterson GH, Lippincott-Schwartz J. A photoactivatable GFP for selective photolabeling of proteins and cells. Science 2002; 297:1873-7.
30. Sandilands E, Cans C, Fincham VJ, Brunton VG, Mellor H, Prendergast GC, et al. RhoB and actin polymerization coordinate Src activation with endosome-mediated delivery to the membrane. Dev Cell 2004; 7:855-69.
31. Macpherson IR, Hooper S, Serrels A, McGarry L, Ozanne BW, Harrington K, et al. p120-catenin is required for the collective invasion of squamous cell carcinoma cells via a phosphorylation-independent mechanism. Oncogene 2007; 26:5214-28.
32. Calautti E, Cabodi S, Stein PL, Hatzfeld M, Kedersha N, Paolo Dotto G. Tyrosine phosphorylation and src family kinases control keratinocyte cell-cell adhesion. J Cell Biol 1998; 141:1449-65.
33. Huen AC, Park JK, Godsel LM, Chen X, Bannon LJ, Amargo EV, et al. Intermediate filament-membrane attachments function synergistically with actin-dependent contacts to regulate intercellular adhesive strength. J Cell Biol 2002; 159:1005-17.
34. Setzer SV, Calkins CC, Garner J, Summers S, Green KJ, Kowalczyk AP. Comparative analysis of armadillo family proteins in the regulation of a431 epithelial cell junction assembly, adhesion and migration. J Invest Dermatol 2004; 123:426-33.